Journal of ELECTRONIC MATERIALS, Vol. 41, No. 3, 2012
DOI: 10.1007/s11664-011-1836-1

Mechanical Strength and Failure Characterization of Sn-Ag-Cu Intermetallic Compound Joints at the Microscale

LEILA LADANI[1,3] and JAFAR RAZMI[2]

1.—Mechanical Engineering Department, University of Alabama, Tuscaloosa, AL 35487, USA.
2.—Civil Engineering Department, University of Maryland, College Park, MD 20742, USA.
3.—e-mail: lladani@eng.ua.edu

Continuous miniaturization of microelectronic devices has led the industry to develop interconnects on the order of a few microns for advanced superhigh-density and three-dimensional integrated circuits (3D ICs). At this scale, interconnects that conventionally consist of solder material will completely transform to intermetallic compounds (IMCs) such as Cu_6Sn_5. IMCs are brittle, unlike conventional solder materials that are ductile in nature; therefore, IMCs do not experience large amounts of plasticity or creep before failure. IMCs have not been fully characterized, and their mechanical and thermomechanical reliability is questioned. This study presents experimental efforts to characterize such material. Sn-based microbonds are fabricated in a controlled environment to assure complete transformation of the bonds to Cu_6Sn_5 IMC. Microstructural analysis including scanning electron microscopy (SEM), energy-dispersive x-ray spectroscopy (EDS), and x-ray diffraction (XRD) is utilized to determine the IMC material composition and degree of copper diffusion into the bond area. Specimens are fabricated with different bond thicknesses and in different configurations for various tests. Normal strength of the bonds is measured utilizing double cantilever beam and peeling tests. Shear tests are conducted to quantify the shear strength of the material. Four-point bending tests are conducted to measure the fracture toughness and critical energy release rate. Bonds are fabricated in different sizes, and the size effect is investigated. The shear strength, normal strength, critical energy release rate, and effect of bond size on bond strength are reported.

Key words: Intermetallics, microelectronics, bonding, mechanical testing, failure

INTRODUCTION

Continuous diminution of electronic interconnects and their ever-increasing density have increased their susceptibility to mechanical and thermomechanical loading and their probability of failure. Introduction of three-dimensional integrated circuits (3D ICs) with demands for bonds less than a few microns thick has introduced challenges for engineers and researchers. New technology based on solid–liquid interdiffusion (SoLID) bonding was recently introduced at the microscale.[1] SoLID bonding, also known as low-temperature transient liquid-phase (LTTLP) bonding[2] or low-temperature (LT) bonding, is preferred over other technologies due to its wide variety of material choices, low temperature, and low cost. The process involves a low temperature melting point (LTM) intermediate material that is deposited on high temperature melting (HTM) substrate. To establish the bond, two pieces of doubly deposited materials' low melting point sides and heat and pressure are applied. The LTM metal is melted, but the HTM metal remains in the solid phase.[3] Solid HTM diffuses into the liquid and reaches the required critical concentration, which results in a phase transformation of the liquid component to higher melting point material,

(Received April 25, 2011; accepted November 24, 2011; published online December 16, 2011)

in most cases intermetallic compounds (IMCs). IMCs are strong enough to serve as a bond and withstand the elevated temperatures to which the package will be exposed during the remaining steps of the packaging and assembly processes (e.g., reflow).[4] However, there are disadvantages in having IMCs in the bond. Conventional solder joints are very ductile and can withstand relatively large amounts of deformation during mechanical and thermomechanical loading without developing large stresses. However, IMCs are typically brittle; therefore, the stresses induced in these bonds during mechanical and thermomechanical loading may be large.

IMCs do not experience the plasticity, creep, and distributed damage that conventional solders experience at room temperature. Therefore, the conventional fatigue and damage modeling techniques (e.g. Coffin–Manson, energy partitioning) that are based on inelastic strain range or plastic and creep strain energy release are not suitable for predicting the fatigue life or number of cycles to failure of IMC materials.

These bonds typically function as electrical, mechanical, and thermal connections, and their failure results in loss of all of these functionalities. Since these interconnects inside the electronic package will experience different types of processing, operation and environmental loading, viz. thermomechanical loads due to reflow process, functional thermal cyclic loads, and environmental temperature variations, vibrations, etc., their mechanical strength and durability is crucial for reliability of electronic devices.

Cu_6Sn_5 is a common IMC that is formed when Sn-based solders are used. Sn-based Pb-free solders are main candidates for replacing Sn-Pb solders due to their process compatibility and reliability. Although extensive research has been conducted on conventional solder joint materials, the behavior of IMCs, including Cu_6Sn_5 and Cu_3Sn, has not been investigated thoroughly. Only limited studies have reported mechanical measurement of Young's modulus and shear strength of Cu_6Sn_5, and even the values reported in these studies present very large scatter.[5,6] Most studies have reported values for joints that are a combination of both IMCs and solder materials. The miniaturization process in modern electronic manufacturing introduces another important factor, size effect, in the properties of solder joints. Size effect has been shown to be a valid concern in Sn-based joints.[7,8] At scales smaller than a few microns, the size of the grains is expected to be on the same order as the bond size, which essentially means that the bond material will behave anisotropically. Additionally, the defect density may be different, which may result in different failure behavior. Material property data obtained from large-scale materials and joints are not valid or reliable for integrity and reliability investigation of joints on the order of a few microns. No study has reported detailed investigation of the size effect on mechanical properties of IMCs as well as the overall performance in real-life application. It is assumed that a significant change in the mechanical behavior of bonds occurs when the size of the solder joint becomes comparable to the grain size.[9] Theoretical evaluations of these properties are also scarce. Only recently have the structural, electronic, and thermoelastic properties of Cu_6Sn_5 been theoretically investigated.[10]

This work presents the experimental procedures that are used to characterize this material and the results obtained for mechanical properties such as bond shear and normal strength, fracture toughness, and size effect.

SPECIMEN FABRICATION AND MECHANICAL TESTING

Four different types of tests were conducted: peeling and double cantilever beam (DCB) tests for normal strength measurements at two different scales, shear test for shear strength measurement at microscale, and four-point bending test for fracture toughness quantification. Figure 1 shows all four test configurations. For experimental feasibility, the bond thickness was on the order of 220 μm for peeling and four-point bending tests, and on the order of 20 μm for DCB and shear tests.

In two tests, the peeling and four-point bending tests, copper was used as substrate. In the other two tests, shear and DCB, zirconia toughened alumina (ZTA) was used as substrate. In the peeling test, $Sn_{3.5}Ag$ solder was deposited manually on a 1-mm-thick, 5-mm-wide copper substrate. Conventional, oxygen-free, high-conductivity copper was used as the high melting point metal. To ensure that the copper surfaces, which are to be bonded, are clean and even, the plates were polished with 1200-grit sandpaper and 1-μm grain size alumina powder. Polishing the copper surface removes impurities

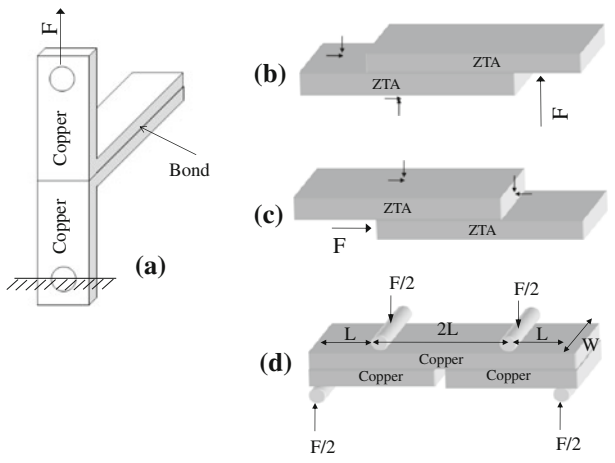

Fig. 1. Test configurations for the four types of tests: (a) peeling test, (b) DCB test, (c) shear test, and (d) four-point bending test. The direction of the force is indicated by an arrow and "F".

and oxide from the surface, provides good contact between copper and solder, and facilitates diffusion of melted $Sn_{3.5}Ag$ into copper and vice versa. After polishing, the copper plates were cleaned with isopropyl alcohol to remove contaminants such as dirt and fingerprints. The copper substrate was bent into an L-shape configuration (Fig. 1) so that fabrication and load application could be carried out conveniently. The solder was deposited in controlled manner with constant volume, and bonds were fabricated using a slight amount of pressure to achieve uniform bond thickness in a thermal chamber. The pressure was adjusted such that the average thickness remained around 220 μm.[1] The fabrication time for complete transformation to Cu_6Sn_5 for this configuration was found to be around 45 min at 260°C.[1]

In fabrication of 3D ICs, the bond thickness may be reduced to 20 μm and even lower, which is much smaller than the size of the bond in the peeling test configuration. To investigate the size effect and evaluate a real application size specimen, another normal test specimen was fabricated in DCB configuration using a more advanced fabrication technique. Copper and $Sn_{3.5}Ag$ material were patterned on a ZTA substrate. ZTA was selected due to its strength and flexural rigidity. Initially, 1000 Å nichrome and 10,000 Å copper were deposited on the ZTA using e-beam depositions. The parts were then taken out of the vacuum system and coated with dry film photoresist, patterned, and developed. Then, the copper was plated to fill in the exposed areas on the substrates. The pattern was then stripped and the base metal etched. The parts were then repatterned to deposit the $Sn\text{-}_{3.5}Ag$ solder alloy through a lift-off procedure. The copper and $Sn\text{-}_{3.5}Ag$ were deposited with 15 μm and 5 μm thicknesses, respectively. An example prebond specimen is shown in Fig. 2. Since the thicknesses of the copper and solder are very small, an exaggerated schematic figure is used to show the side view. The ZTA was 15 mm wide. To increase the stress level during the test, the bonded area had total width of 3 mm (1.5 mm on each side).

The bonding process was conducted in the laboratory using an integrated Instron Micro-tester and a custom-built thermal chamber. The pieces were placed in contact, and heat was applied for 10 min at 260°C to form the bonds. It was found that the final bond thickness varied mainly because of variations in solder paste thickness, and that the copper layer which was 15 μm thick was consumed or became indistinguishable from the bond itself. The average bond thickness was found to be around 20 μm. Temperature of 260°C was found to be optimal for complete transformation to Cu_6Sn_5 material[1] for 20 μm bond thickness. Microstructural analysis was conducted for both the peeling test and DCB specimens to confirm complete transformation to IMCs.

DCB and shear test specimens were fabricated using ZTA samples according to the configurations shown in Fig. 1.

A four-point bending test with a notched specimen, a very common configuration used for measuring fracture toughness and critical strain energy release rate, was conducted using copper plates bonded using a thick layer (average 220 μm) of IMC material. This test requires a precrack in the bond at the notch. The precrack was created manually using a microblade. Since creating this precrack for bond thickness of 20 μm is extremely difficult, the four-point bending test was only conducted for the larger-scale bond.

The advantage of using this technique is that it is not necessary to know the size of the precrack in order to calculate the critical energy release rate as long as the crack is within the constant moment region of the specimen. The critical energy release rate can be calculated from the following equation:

$$G = \frac{M^2(1-v^2)\left(\frac{1}{I_c}-\frac{1}{I_2}\right)}{2E} = \frac{21(1-v^2)M^2}{4Eb^2h^3}, \quad (1)$$

where M is the net bending moment and is equal to $\frac{FL}{2}$, F is the plateau load, L is the distance between the inner and outer loading points, v is the Poisson's ratio of the bulk substrate, E is the elastic modulus of the bulk substrate, and I_2 and I_c are the moments of inertia per unit cross-section for the lower layer and composite beam, respectively. b and h are the width and thickness of the layers (assuming equal thicknesses and equal widths for both top and bottom layers).

The specimen length was 26 mm, and the spans of the supports and the inner loading points were 16 mm and 26 mm, respectively. The specimen was loaded in a four-point bending test fixture and subjected to loading increments using the Instron Micro-tester. The load versus displacement characteristic was monitored, and the critical load for crack propagation was recorded from the load drop observed in the curve.

All of the mechanical characterization tests were conducted using the Instron Micro-tester. The machine is equipped with capacitive gauges that are used to determine the displacement at the gauge length with resolution of 0.3 μm (Figs. 3, 4).

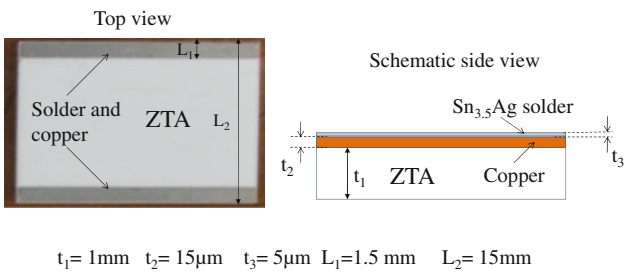

t_1= 1mm t_2= 15μm t_3= 5μm L_1=1.5 mm L_2= 15mm

Fig. 2. Top view and schematic side view of prebond specimens for DCB and shear tests.

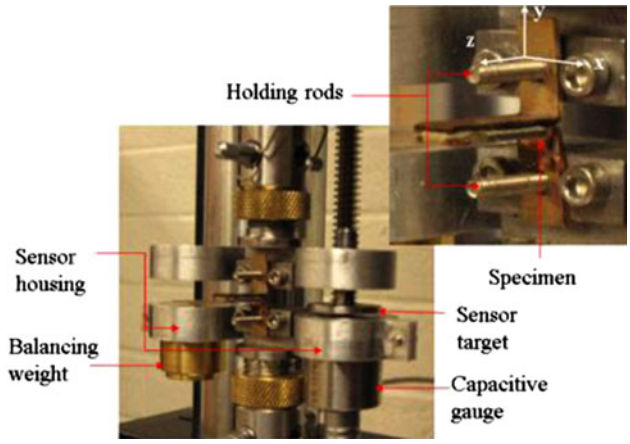

Fig. 3. Test fixture used, interfaced with the Instron Micro-tester to measure bonding strength in the peeling test.

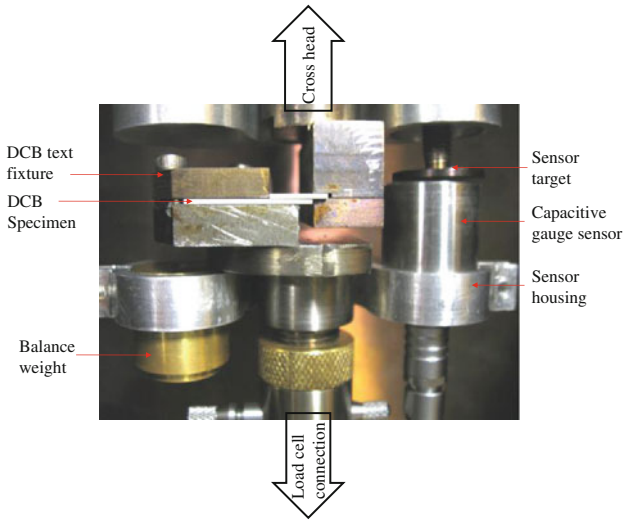

Fig. 4. Test fixture and configuration for DCB test.

A fixture with submicron tolerances was specifically designed for this test. The fixture houses the capacitive gauge and facilitates measurement of accurate deformation within the gauge.[11] Blue Hill software was used to collect and analyze the data. At least five specimens were fabricated and tested for each test configuration to obtain statistically significant data.

MICROSTRUCTURAL ANALYSIS

SEM and EDS analyses were utilized to determine the extent of copper diffusion and transformation of the bond to Cu_6Sn_5. The minimum amount of copper required for this transformation is 39 wt.%. EDS analysis showed the percentage of copper to be about 39% in the middle of the bond. An example SEM image of the bond is shown in Fig. 5. It appears that the lower copper layer has been dissolved completely into the bond.

Posttest failure analysis was also conducted using an optical microscope. A fractured surface is shown in Fig. 6. A dimple-like fracture surface is observed in this figure. The analysis shows fracture surface features on the order of 10 μm. The fractured surface features show an intergranular type of fracture, indicating weak grain boundaries and embrittlement. The size of a single grain appears to be around 10 μm, as seen in Fig. 6. This is comparable to the size of the bond in the case of the DCB test. XRD analysis was also conducted. One example is shown in Fig. 7. Cu_6Sn_5 is the major component in the bond area. This analysis was conducted on the fractured surface. Cu_3Sn was also observed in both large and small specimens. The thickness of Cu_3Sn was measured to be around 300 nm in DCB test samples and around 1 μm in peeling test sample. These layers were observed adjacent to the copper layer. However, the failure occurred in the middle of the bonds in Cu_6Sn_5 layers and away from Cu_3Sn layers.

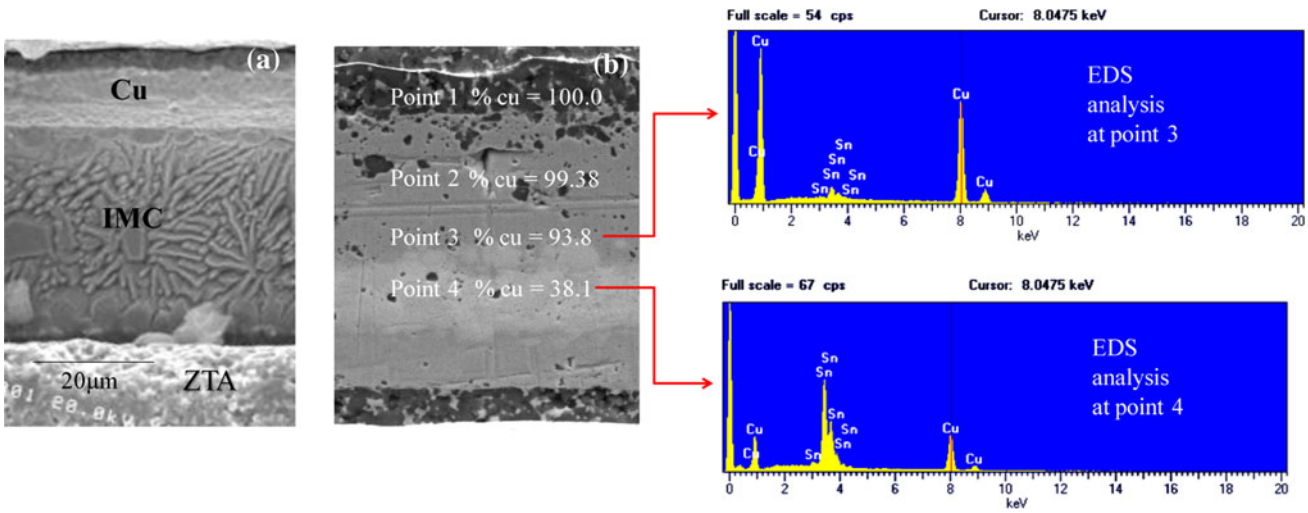

Fig. 5. (a) SEM image of the SoLID bond (the scale bar is the same in both figures) and (b) EDS analysis of the percent copper in the bond.

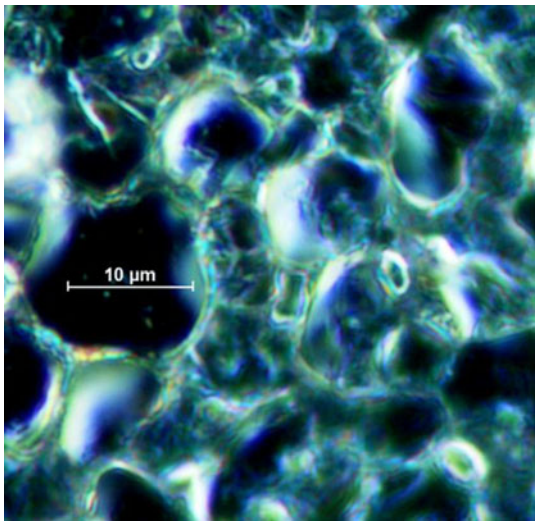

Fig. 6. Fractography of a failed DCB specimen.

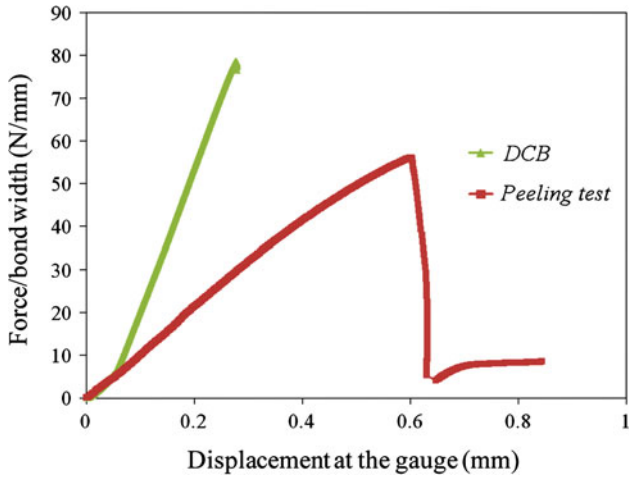

Fig. 8. Normal strength measured using peeling test and DCB configuration.

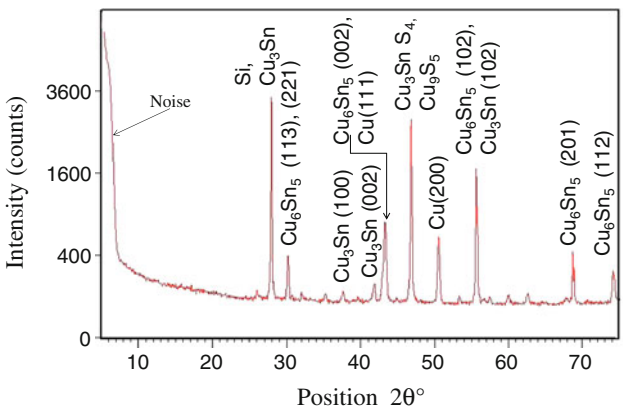

Fig. 7. XRD pattern of the IMC specimen.

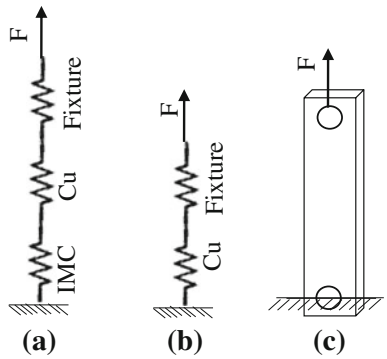

Fig. 9. (a) 1D analytical representation of displacement at the gauge in the peeling test, (b) 1D analytical representation of displacement at the gauge for compliance correction test, and (c) schematic view of compliance correction test.

EXPERIMENTAL RESULTS

Load–displacement data were collected in the peeling, DCB, shear, and four-point bending tests. The maximum load at failure was accurately measured by the Instron Micro-tester. Figure 8 shows example load–displacement curves for the peeling and DCB test configurations. In both DCB and peeling tests, the stress is maximum at the edge where the crack starts and decreases with distance from the edge. Since the force is not applied uniformly to the surface, the concept of stress is not used here. The value of bond strength can simply be represented by the force; however, since the dimensions of these two test specimens are different (test specimens have different width), force per unit length is used to compare the results of the two tests.

At this scale, it is not possible to mount a strain gauge on the specimen. Even with other techniques of strain measurement typically used at smaller scales such as digital image correlation or video extensometers, it is cumbersome to observe strain on the bond area itself under the shadow of substrates. In many specimens, the slight depth of the bond relative to the substrate level makes focusing very difficult. One solution would be to polish the surface before testing, but this may damage the bonds at this small scale. Additionally, constant movement of the specimen during the test causes the bond area to move out of the focus of the camera, making it extremely difficult to compare sequential images taken from a specimen.

In these tests, the displacement within the gauge length was measured using a capacitive gauge. However, this deformation within the gauge length is not an accurate measurement of bond strain; for example, in the peeling test, this measurement includes the total deformation of copper (elastic and plastic deformation at pin holes), fixture deformation, tolerances, and errors. A one-dimensional analytical model representing the total deformation measured by the capacitive gauge can clearly illustrate this issue, as seen in Fig. 9.

According to Fig. 9a,

$$\Delta l_{\text{Tot}} = \Delta l_{\text{IMC}} + \Delta l_{\text{Cu}} + \Delta l_{\text{Fixture}} + \text{Error}, \quad (2)$$

where Δl_{Cu} is the elastic and plastic deformation of the copper. To isolate the deformation in the IMC, a compliance correction test was conducted in which a piece of copper with the same dimensions as the copper substrate in the peeling test and length equal to the sum of the lengths of the copper handles in the L-shaped substrate was tested under tension in the same manner as the peeling test was conducted. If the error and noise caused by the fixture tolerances are insignificant compared with the IMC deformation, then the difference between the peeling test and compliance correction tests should be roughly equal to the deformation in the IMC material. The results of peeling and compliance correction tests were compared. However, the difference between the two tests was found to be within the observed error range. The conclusion from this analysis is that the deformation in the IMC material is smaller than the resolution of the system. Therefore, it is not possible to obtain accurate strain results from this test.

The bond thicknesses in both the peeling and DCB tests are much smaller than the gauge length, and measuring strain directly on the bonds is virtually impossible with conventional strain measurement techniques. Because of this difficulty, in this study we do not rely on strain measurements to extract fracture strain or other mechanical characteristics such as Young's modulus. There is much less error in strength (load) measurement using the Instron Micro-tester. The variation between different specimens is small, and therefore repeatable and reliable results were obtained for different specimens. Therefore, this study only focuses on measuring strength and characterizing failure at different scales.

The results show that the normal strength obtained in the DCB test is higher than that in the peeling test, showing a possible effect of size. The most likely explanation for the observed dependence of the mechanical behavior (normal strength) of the IMCs on the joint size (thickness) could be attributed to several factors including lower number of grains and lower density of grain boundaries. Grain boundaries are sources of stress concentration, and reduction of their density can delay failure. Furthermore, as the bond side decreases, the number of defects decreases, resulting in lower probability of crack initiation and failure. Furthermore, the thickness of IMC is much higher in the large-scale specimen than in the small-scale specimen. Higher thickness has been shown to attribute to lower strength. Higher thickness results in coarser interfaces, resulting in more jagged grains that act as sources of stress concentration and points of crack initiation.[12]

The brittle nature of the failure is apparent in both the large-scale and small-scale tests from the sudden load drop observed at failure. This indicates that, immediately after the crack initiates at failure, it instantaneously propagates through the joint and results in complete failure. Fractography analysis indicates that the failure occurs closer to the center of the bond, where the major IMC is Cu_6Sn_5. Microstructural analysis of the bonds shows a thin layer of Cu_3Sn (300 nm thick in DCB specimens, 1 μm in peeling test specimens) adjacent to the copper layer. The fact that the failure did not occur at Cu_3Sn or the interface of Cu_3Sn and Cu_6Sn_5 shows that the Cu_6Sn_5 compound is the most vulnerable part of the IMC. In other words, Cu_3Sn is possibly stronger than Cu_6Sn_5. Stress analysis of multilayer IMCs showed that high stress concentration occurs in the hardest element of the IMCs.[12] The hardness of Cu_6Sn_5 was found to be higher than that of Cu_3Sn (3.7 GPa for Cu_6Sn_5 versus 3.36 GPa for Cu_3Sn). Additionally, Cu_6Sn_5 demonstrates lower fracture toughness than Cu_3Sn. Therefore, it is more favorable for the crack to initiate and propagate in Cu_6Sn_5 than in Cu_3Sn.[12]

In this analysis we are dealing with IMC layers with significantly higher thickness compared with regular solder joints. As the IMC thickness increases, the morphology of the IMC changes and rougher interfaces are expected. Additionally, the volume reduction which is caused by transformation of solder material to IMCs causes residual or "misfit" stresses[12] within IMC layers. This residual stress along with the low fracture toughness of the Cu_6Sn_5 results in failure of this IMC.

Shear test data were also collected. The maximum shear strength was found to be on average about 70 MPa, as seen in the example shown in Fig. 10. The sharp load drop observed in the peeling and DCB tests was not observed in the case of shear. This is mainly attributed to the fact that large friction exists between the top and bottom layers after failure. Due to this large friction, the

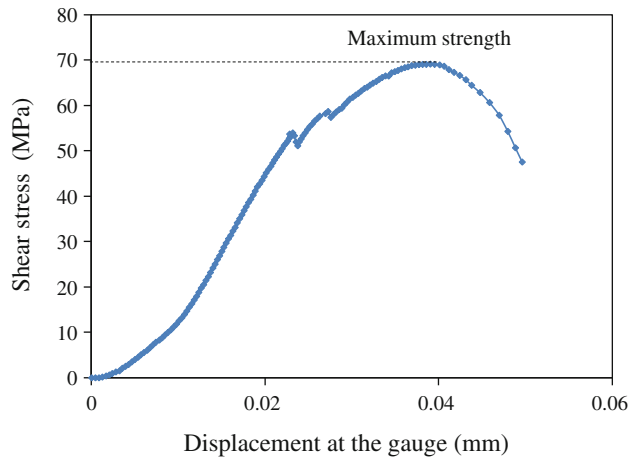

Fig. 10. Example of shear test data collected.

Table I. Material properties in the four-point bending test

Material	Copper	Cu_6Sn_5
Elastic modulus, E (GPa)	117	59–125[4,12–14]
Poisson ratio, ν	0.34	0.29

morphology of the failed surfaces is distorted and, therefore, is not a reliable target for fractography.

In terms of stress concentration, the same analysis is valid in the shear stress case. Again, the maximum stress occurs in the Cu_6Sn_5 layer. The posttest microstructural analysis confirmed failure in this layer. The value of the shear strength observed in this analysis is comparable to the literature.[12]

In four-point bending test the critical load value, which indicates the occurrence of crack growth, was specified based on the sudden drop in the load value. It was found that a critical four-point load of 42.5 N caused a notched specimen to experience crack propagation through the interface. The critical load value and mechanical and dimensional data of Table I and Eq. 1 were used to evaluate the critical energy release rate, whose value was found to be 38.47 J/m^2. Based on the range of values for elastic modulus found in literature, this value of strain energy release rate translates into a fracture toughness value in the range from 1.5 MPa m$^{1/2}$ to 2.2 MPa m$^{1/2}$. This fracture toughness value is very close to the typical values for most brittle materials.

CONCLUSIONS

Four different types of test were conducted in this study to experimentally characterize the mechanical behavior of Cu_6Sn_5 material. Peeling and DCB tests were performed at different scales and showed that the normal strength of IMC joints may be affected by bond size, with higher strength at smaller scale. This effect could be attributed to the lower number of defects and lower density of grain boundaries. Other possible effects may include the rougher morphology of thicker IMC layers in large specimens, which causes stress concentration at grain interfaces and causes faster crack initiation in larger joints. Shear strength is also reported here to be 70 MPa on average. In all of the tests, failure was observed in the Cu_6Sn_5 layer. Four-point bending tests showed a very consistent value of fracture toughness for IMC material compared with common values for brittle-type materials in literature. Microstructural analysis was also performed. SEM and EDS revealed detailed charts that show the amount of copper which is required to be diffused into the bond area to produce Cu_6Sn_5. XRD analysis also shows that the major constituent of the IMC bond is Cu_6Sn_5. Posttest failure analysis provides clear pictures of fracture surface features on the order of the grain size for bond sizes on the order of 20 μm.

REFERENCES

1. L. Ladani, J. Razmi, and J. Bentley, *Thin Solid Films* 518, 4948 (2010).
2. M.M. Hou and T.W. Eagar, *J. Electron. Packag.* 114, 443 (1992).
3. J.C. Lin, L.W. Huang, G.Y. Jang, and S.H. Lee, *Thin Solid Films* 410, 212 (2002).
4. F. Bartels, J.W. Morris, G. Dalke, and W. Gust, *J. Electron. Mater.* 23, 8 (1994).
5. R.J. Field and S.R. Low, *Physical and Mechanical Properties of Intermetallic Compounds Commonly Found in Solder Joints* (National Institute of Standards and Technology, 2011). http://www.metallurgy.nist.gov/mechanical_properties/solder_paper.html.
6. J.O.G. Parent, D.D.L. Chung, and I.M. Bernstein, *J. Mater. Sci.* 23, 2564 (1988).
7. P. Zimprich, A. Betzwar-Kotas, G. Khatibi, B. Weiss, and H. Ipser, *J. Mater. Sci.* 19, 383 (2008).
8. L.M. Yinm, X.P. Zhang, and L.U. Chunsheng, *J. Electron. Mater.* 38, 2179 (2009).
9. E. Arzt, *Acta Metall. Mater.* 46, 5611 (1998).
10. W. Zhou, L. Liu, and P. Wu, *Intermetallics* 18, 922 (2010).
11. L. Ladani, J. Razmi, and J. Carter, U.S. patent 12/611,189. Patent application, Nov 3, 2009.
12. H.T. Lee, M.H. Chen, H.M. Jao, and T.L. Liao, *Mater. Sci. Eng. A Struct.* 358, 134 (2003).
13. R. Agrawal, B. Peng, E.E. Gdoutos, and H.D. Espinosa, *Nano Lett.* 8, 3668 (2008).
14. G.H. Jang, J.W. Lee, and J.G. Duh, *J. Electron. Mater.* 33, 1103 (2004).